

## Mixing of nano-particles by rapid expansion of high-pressure suspensions

JUN YANG, YULU WANG, RAJESH N. DAVE\* and ROBERT PFEFFER

*New Jersey Center for Engineered Particulates (NJCEP), New Jersey Institute of Technology, University Heights, Newark, NJ 07102-1982, USA*

Received 31 January 2003; accepted 3 April 2003

**Abstract**—The mixing of two different species of nano-particles using an environmentally benign technique called rapid expansion of high-pressure suspensions (REHPS) has been studied experimentally. Comparative experiments were also performed by mixing the nano-particles in an organic solvent under ultrasonic agitation and in a dry mechanical mixing process called magnetically assisted impaction mixing. Various characterization methods for evaluating the degree of mixing at length scales of about  $1\ \mu\text{m}$  and lower based on electron microscopy are also described. An analysis of the experimental results indicates that the REHPS mixing, which also includes supercritical conditions, provides results that are significantly better than those of the other two mixing methods considered. It appears that the sudden decrease in pressure in the REHPS process breaks up the nano-particle agglomerates and results in good mixing, especially when the two constituents do not vary significantly in density. The characterization results show that field emission scanning electron microscopy can be used for distinguishing mixtures at the nano-scale if a significant difference in size or shape exists. However, in general, electron energy loss spectrography is the most powerful method to characterize nano-particles mixtures as it maps elemental distribution at nanometer resolution. Energy dispersive X-ray spectroscopy can also be used as a cheap and simple semi-quantitative method to measure the degree of mixing.

**Keywords:** Mixing; nano-particles; characterization; rapid high-pressure expansion; energy dispersive X-ray spectroscopy; field emission scanning electron microscopy; electron energy loss spectrography; magnetically assisted impaction mixing; solvent-based mixing.

### 1. INTRODUCTION

Powder mixing is widely used in the chemical, pharmaceutical, food, cosmetic and pigment industries, and, thus been the subject of intense research during the past 10 years [1, 2]. However, most research in this field has been limited to large, non-cohesive, spherical particles and rarely includes micron- or submicron-sized

---

\*To whom correspondence should be addressed. E-mail: [dave@adm.njit.edu](mailto:dave@adm.njit.edu)

particles. Recently, due to the increasing emphasis on research and development of nano-structured materials, nano-particle mixing has become important due to potential new applications of nano-composites [3]. However, two major problems need to be solved for nano-particle mixing, i.e. how to mix them well [4–6] and how to characterize the degree of mixing at the nano-scale [7–9].

Since nano-particles are always agglomerated due to their large interparticle forces, de-agglomeration is the first step necessary for obtaining a good mixture. For commonly used dry mechanical mixers, either intense shear or high velocity impacts, or both, are needed to de-agglomerate and mix the particles. In previous work by our group, several mechanical mixing devices were utilized to mix nano-particles with varying results [10]. In this paper, we concentrate on mixing nano-particles by the rapid expansion of supercritical (or liquid, at very high pressure) suspensions (REHPS) and compare the results with those obtained using a mechanical mixing device and the magnetically assisted impaction mixer (MAIM). The MAIM process was developed in our laboratory and is based on the magnetically assisted impaction coater (MAIC) patented by Aveka (Minnesota, USA). Control experiments were also carried out using an organic solvent in which the nano-particle suspension is subjected to ultrasonic agitation.

Our investigation is also concerned with the problem of evaluating the degree of mixing at the nano-scale, which is essentially a new area of research. Traditional mixing measurement methods (for larger particles) such as a colorimeter image analysis system [7] or an electrostatic effect analysis system [8] cannot be used to obtain nano-scale resolution data for quantitative characterization. In this study, two different length-scale characterization methods were used. Energy dispersive X-ray spectroscopy (EDX) was used as a micron-size analysis tool, while field emission scanning electron microscopy (FESEM) and electron energy loss spectroscopy (EELS) were used to evaluate the degree of mixing at length scales as small as 100 nm.

## 2. EXPERIMENTAL

### 2.1. Powders

Five different nano-particles were used to study mixing performance. (i) Molybdenum trioxide, U2, crystallized particles produced by Climax Molybdenum with a specific surface area of  $35 \text{ m}^2/\text{g}$  and an average size of about 20–70 nm. A FESEM analysis shows that the size distribution is very wide, including many micron-sized flakes. (ii) Nano copper particles supplied by Argonide with a specific surface area of  $5\text{--}8 \text{ m}^2/\text{g}$  and an average size of 100–150 nm. The particles are spherical, produced by the electro-exploded wire technique and then passivated with air to form a coating of copper oxide. (iii) Aerosil R972 silica supplied by Degussa with a specific surface area of  $114 \text{ m}^2/\text{g}$ . A transmission electron microscopy (TEM) analysis indicates an average particle size of about 25 nm in a chain-like structure.

- (iv) Aluminium oxide C, also supplied by Degussa, with a specific surface area of  $110 \text{ m}^2/\text{g}$ . A TEM analysis indicates an average particle size of about 13 nm.
- (v) Titanium dioxide P25, also supplied by Degussa, with a specific surface area of  $48 \text{ m}^2/\text{g}$  and an average particle size of about 28 nm.

## 2.2. Mixing methods

**2.2.1. REHPS mixing.** Figure 1 is a schematic diagram of the first REHPS mixing apparatus that we used in our experiments. It consists of a 1000-ml high-pressure vessel with depressurization of the suspension occurring at the top of the high-pressure vessel (called top release). This top-release apparatus is capable of achieving pressures up to  $1.724 \times 10^7 \text{ Pa}$  and a stirring speed of 800 r.p.m. As will be shown later, this apparatus produced results with limited success. We also used a second similar apparatus (300-ml high-pressure vessel) with depressurization of the suspension occurring at the bottom of the high-pressure vessel (called bottom release). This second apparatus is capable of achieving pressures up to  $4.137 \times 10^7 \text{ Pa}$  and a stirring speed of 3000 r.p.m.

In the top-release apparatus a mixture of  $\text{Al}_2\text{O}_3/\text{SiO}_2$  (1:1, by weight),  $\text{Al}_2\text{O}_3/\text{MoO}_3$  (1:1) or  $\text{Cu}/\text{TiO}_2$  (2:1) was loaded into the 1000-ml REHPS reactor and then  $\text{CO}_2$  was pumped in until the pressure reached a specified value. The temperature of the water bath was set at  $40^\circ\text{C}$ . Before depressurization (top release) the suspension was stirred for 20 min at 100 r.p.m. and released through a nozzle of diameter  $500 \mu\text{m}$ . Samples were collected in the collector tank (see Fig. 1) with the release pressure carefully controlled.

In another series of experiments, a mixture of nano  $\text{Al}_2\text{O}_3/\text{SiO}_2$  (1:1, by weight),  $\text{Al}_2\text{O}_3/\text{MoO}_3$  (1:2) or  $\text{Cu}/\text{TiO}_2$  (3:1) was loaded into the 300-ml bottom-release

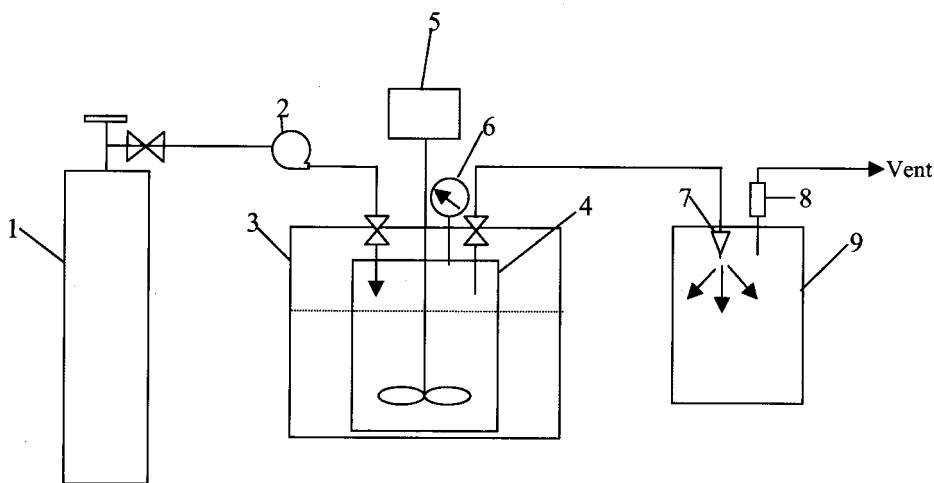


**Figure 1.** Set-up of the top-release REHPS mixer. 1,  $\text{CO}_2$  cylinder; 2,  $\text{CO}_2$  pump; 3, water bath; 4, high-pressure vessel; 5, agitator; 6, pressure gauge; 7, nozzle; 8, filter; and 9, collector vessel.

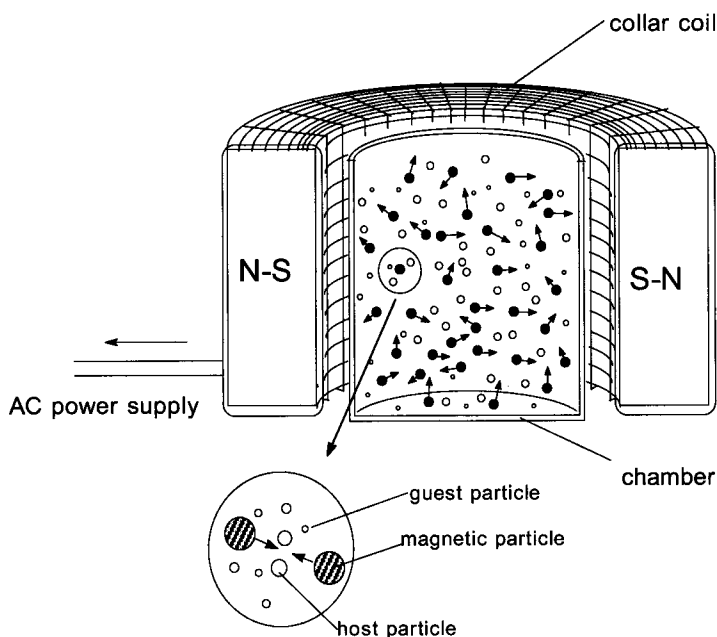


**Figure 2.** Experimental set-up of the MAIM system.

REHPS reactor and then  $\text{CO}_2$  was pumped in until the pressure reached a specified pressure. The temperature was kept at  $42.5^\circ\text{C}$ . The suspension was stirred for 20 min at 1000 r.p.m. and then released through either a 500- or 250- $\mu\text{m}$  diameter nozzle. Samples were once again collected in the collector tank with the release pressure carefully controlled.

**2.2.2. MAIM mixing.** A mixture of nano  $\text{Al}_2\text{O}_3/\text{SiO}_2$  (1 : 1),  $\text{Al}_2\text{O}_3/\text{MoO}_3$  (1 : 1) or  $\text{Cu}/\text{TiO}_2$  (3 : 1) was poured into a 200-ml glass bottle and processed for 15 min. The size range of the magnets used was 1.4 to 1.7 mm and the mass ratio of powder mixture to magnets was 1 : 12. A schematic diagram of the MAIM apparatus used is shown in Fig. 2.

**2.2.3. Solvent-based mixing.** A mixture of nano  $\text{Al}_2\text{O}_3/\text{SiO}_2$  (1 : 1),  $\text{Al}_2\text{O}_3/\text{MoO}_3$  (1 : 1) or  $\text{Cu}/\text{TiO}_2$  (3 : 1) was dispersed into 40 ml of hexane and the suspension placed in an ultrasonic bath (100 W, 20 kHz) for 20 min. The solution was filtered and dried at  $80^\circ\text{C}$  for 24 h to obtain dry samples.

### 3. CHARACTERIZATION OF THE MIXING OF NANO-POWDERS

The characterization of nano-particle mixtures requires high-resolution instruments that can image particles down to the nano-scale. SEM and TEM were utilized for this task.



### 3.1. FESEM

We used a JEOL 6335F and a LEO 982 capable of obtaining a high magnification image and enabling us to differentiate nano-particles by their shape or size. In addition, the ratio of the two metallic elements in a mixture of metals and/or metal oxides can be obtained by analyzing a micro area or spot of around  $1\ \mu\text{m}$  in diameter on the sample surface with an EDX detector. A small amount of the powder samples was randomly dispersed onto a piece of carbon tape for analysis by EDX. A comparison of the atomic ratio of the two metallic elements obtained from many randomly chosen spots along the sample surface would indicate the degree of homogeneity of the sample. If enough data points are collected, a standard deviation can be calculated. By comparing the standard deviation obtained from different samples, a fairly reliable indicator can be obtained for evaluating the degree of mixing of the sample at the micron scale. Also, an EDX mapping of the elemental distribution in the samples can directly demonstrate the homogeneity (or in-homogeneity) of the mixture.

### 3.2. Scanning TEM (STEM)

STEM (LEO 922) requires preparation of very thin samples, which were prepared by blowing a small amount of powder directly onto the TEM sample grid. Due to the very light/thin samples used and a higher resolution than FESEM, it was easier to detect different nano-particles in the images by their size and shape. Moreover, by using EELS along with STEM, mapping of selected elements can be observed directly. As will be shown in the results, this is a powerful tool to study the degree of mixing of nano-particle mixtures at high resolution.

## 4. RESULTS AND DISCUSSION

### 4.1. Evaluation of mixing methods: top-release REHPS apparatus

In the first series of experiments, the mixture of  $\text{Al}_2\text{O}_3/\text{SiO}_2$  (1 : 1) was processed by various mixing methods, including REHPS using the top-release apparatus. In order to evaluate each of the mixing methods, an EDX spot analysis was run. For each sample imaged, at least 20 spots were randomly chosen and the results were statistically analyzed. The results are shown for the three different mixing methods in Fig. 3, where the distribution of the atomic ratio of Al/Si is plotted against the frequency of occurrence. In these plots, a sharp single peak in the frequency plot corresponds to better mixing. The plots shown indicate that the top-released REHPS mixture (here we collected the sample during the time interval when the pressure in the reactor dropped from  $1.379 \times 10^7$  to  $8.274 \times 10^6$  Pa) gives only one peak, which is also very close to the theoretical Al/Si ratio (1.1344), while the other three mixtures all show more than one peak, which means that the distribution of the two components is not very uniform. When the standard deviation of the data for

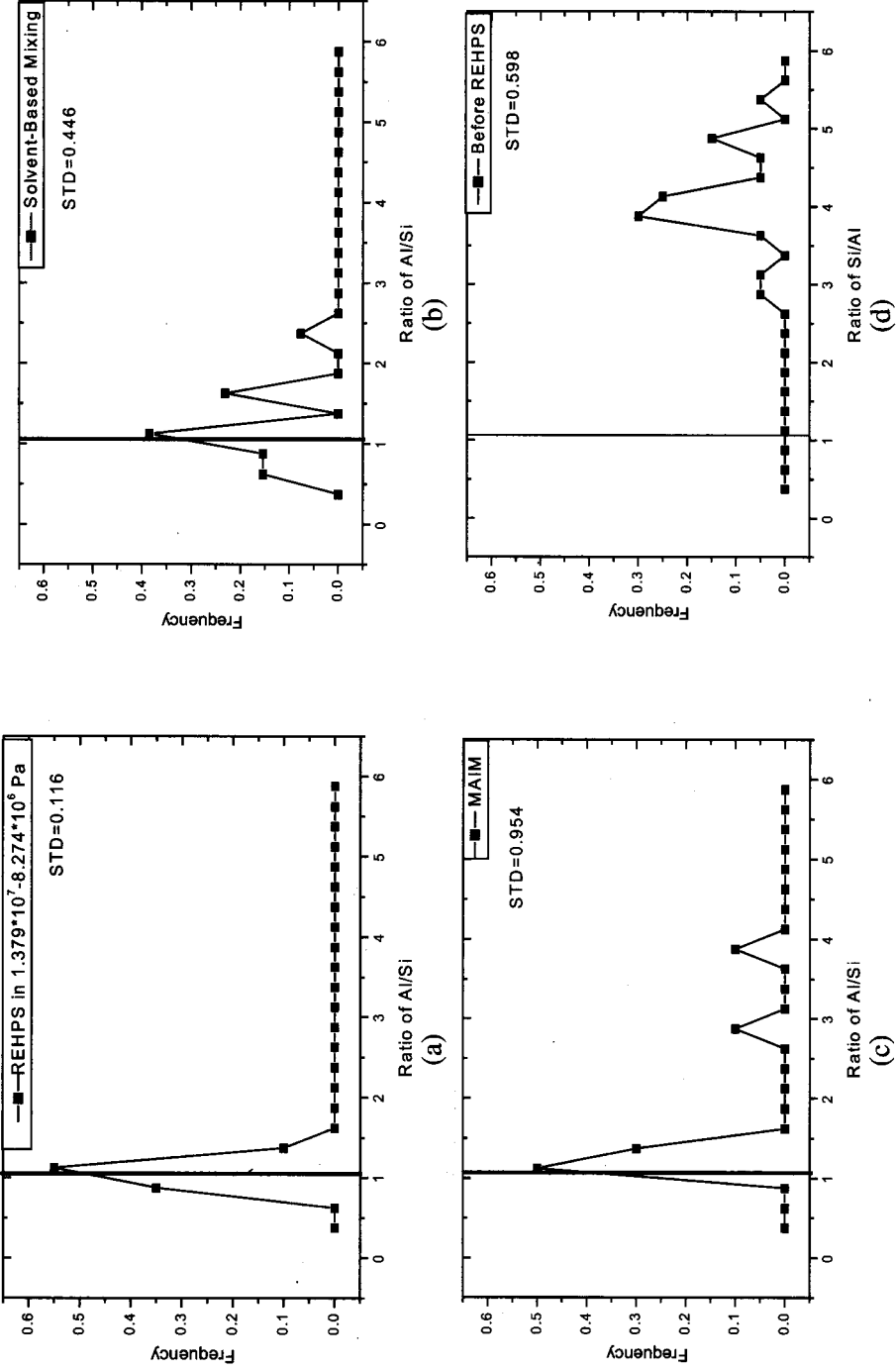


**Figure 3.** EDX spot analysis results of the mixtures of  $\text{SiO}_2/\text{Al}_2\text{O}_3$  (1:1). Results for (a) REHPS, released while the pressure in the chamber dropped from  $1.379 \times 10^7$  down to  $8.274 \times 10^6$  Pa, (b) solvent-based mixing, (c) MAIM mixing and (d) supercritical fluid stirring without rapid pressure expansion.

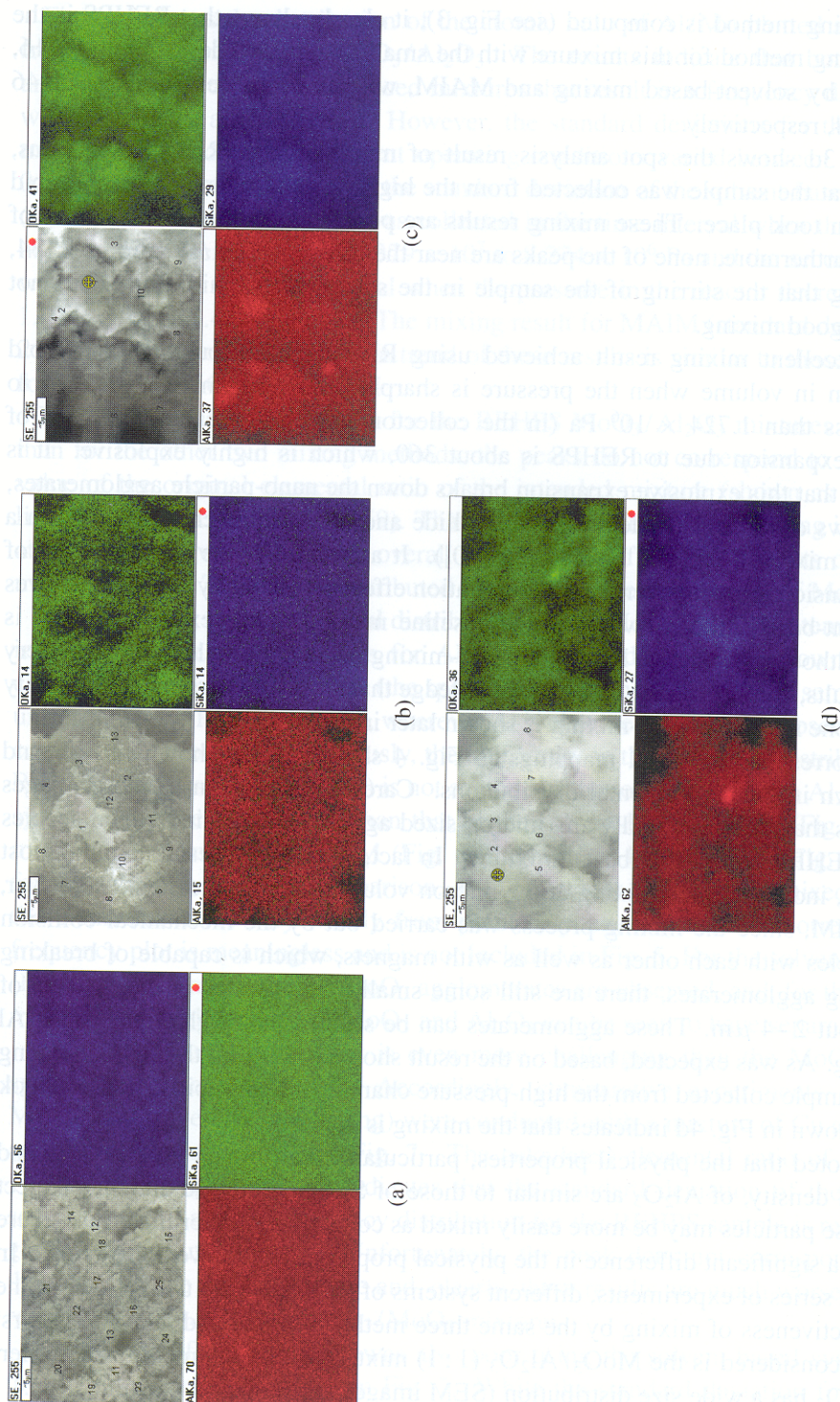


**Figure 4.** EDX mapping of the mixtures of  $\text{Al}_2\text{O}_3/\text{SiO}_2$ . Results in each case show secondary electron image (top left), Al map (bottom left) and S map (bottom right) for (a) REHPS, released while pressure in the chamber dropped from  $1.379 \times 10^7$  down to  $8.274 \times 10^6$  Pa, (b) solvent-based mixing, (c) MAIM mixing and (d) supercritical fluid stirring without rapid pressure expansion. This figure is published in colour on <http://www.ingenta.com>.

each mixing method is computed (see Fig. 3), it clearly shows that REHPS is the best mixing method for this mixture with the smallest standard deviation of 0.116, followed by solvent-based mixing and MAIM, with standard deviations of 0.446 and 0.954, respectively.

Figure 3d shows the spot analysis result of mixing in the REHPS apparatus, except that the sample was collected from the high-pressure chamber before rapid expansion took place. These mixing results are poor, with a standard deviation of 0.598. Furthermore, none of the peaks are near the theoretical Al/Si ratio of 1.134, indicating that the stirring of the sample in the supercritical fluid alone does not produce good mixing.

The excellent mixing result achieved using REHPS is attributed to the rapid expansion in volume when the pressure is sharply reduced from  $1.379 \times 10^7$  to much less than  $1.724 \times 10^6$  Pa (in the collector tank). The calculated ratio of volume expansion due to REHPS is about 360, which is highly explosive. It is believed that this explosive expansion breaks down the nano-particle agglomerates, and allows different particle species to collide and mix with each other to form a uniform mixture (e.g. see Fig. 14b in [10]). It appears that the mixing effect of this expansion is even better than the cavitation effect produced by ultrasonic waves in solvent-based mixing, which is the baseline method in our experiments. It is noted (although not shown here) that hand-mixing of nano-particles produced very poor results, confirming the common knowledge that these powders cannot be easily mixed (one result for hand-mixing is shown later in Fig. 6).

The corresponding EDX mappings in Fig. 4 show the Al (shown in red) and Si (shown in green) elemental distributions. Careful observation of these images indicates that there are hardly any micron-sized agglomerates of individual species in the REHPS and solvent-based mixtures. In fact, the REHPS results are the most uniform, indicating that mixing at the micron volume scale is excellent. However, for MAIM, since the mixing process was carried out by the mechanical collision of particles with each other as well as with magnets, which is capable of breaking down big agglomerates, there are still some small agglomerates in the mixture of size about 2–4  $\mu\text{m}$ . These agglomerates can be seen as the bright spots in the Al mapping. As was expected, based on the result shown in Fig. 3d, the EDX mapping of the sample collected from the high-pressure chamber before rapid expansion took place shown in Fig. 4d indicates that the mixing is poor.

It is noted that the physical properties, particularly the primary particle size and material density, of  $\text{Al}_2\text{O}_3$  are similar to those of  $\text{SiO}_2$ . Therefore one may expect that these particles may be more easily mixed as compared to other materials where there is a significant difference in the physical properties of the two constituents. In the next series of experiments, different systems of particles were used to determine the effectiveness of mixing by the same three methods considered above. The first system considered is the  $\text{MoO}_3/\text{Al}_2\text{O}_3$  (1 : 1) mixture where, as mentioned earlier, the  $\text{MoO}_3$  has a wide size distribution (SEM images are shown to illustrate this).

Figure 5 shows the distribution of the atomic ratio of Al/Mo plotted against the frequency for mixtures of  $\text{MoO}_3/\text{Al}_2\text{O}_3$ . The results indicate that both REHPS and solvent-based mixing produced mixtures that result in a frequency distribution with essentially a single peak. However, the standard deviations for the REHPS mixture collected at two different operating conditions varied between 0.157 and 0.117, and are both smaller than the standard deviation of the solvent-based mixture (0.562). Here the first sample was collected in the time interval when the pressure in the reactor decreased from  $1.379 \times 10^7$  to  $8.274 \times 10^6$  Pa and the second sample was collected in the time interval when the pressure in the reactor decreased from  $1.034 \times 10^7$  to  $3.447 \times 10^6$  Pa. The mixing result for MAIM (standard deviation of 2.858) is quite poor. Overall, the trend of these results is similar to those obtained for the  $\text{Al}_2\text{O}_3/\text{SiO}_2$  system.

While the standard deviations for the REHPS  $\text{MoO}_3/\text{Al}_2\text{O}_3$  mixtures are lower than for the other two mixing methods, the peaks do not correspond to the actual value of the original elemental ratio of the intended mixture (shown as a vertical line at a calculated value of 1.259). That means that although the mixing is uniform at the micron level, there is an overall stratification of the constituents during the mixing process. This may be attributed to the wide size distribution of  $\text{MoO}_3$ .

EDX mapping of the elemental distribution for the  $\text{MoO}_3/\text{Al}_2\text{O}_3$  system is shown in Fig. 6. Here, the mappings for Al (shown in red) and Mo (shown in blue) correspond well with each other (the spatial distribution of the mixture sample is not uniform, but for REHPS mixing, wherever Al is observed, Mo is also observed at the corresponding location). Obviously, the uniformity in the elemental distribution for REHPS mixtures (Fig. 6a and b) is not as good as that observed for the  $\text{Al}_2\text{O}_3/\text{SiO}_2$  system. However, it is better than that of the solvent-based mixing (Fig. 6c), and much better than that of MAIM (Fig. 6d) as well as hand-mixing (Fig. 6e) done for the sake of a baseline comparison. It is noted that for the hand-mixed sample, the elemental ratios vary widely from point to point, and hence a corresponding frequency plot is meaningless and is not included in Fig. 5. For the solvent mixture (Fig. 6c), small micron-sized  $\text{MoO}_3$  agglomerates are observed, and, for the MAIM mixture, big agglomerates of  $\text{MoO}_3$  and  $\text{Al}_2\text{O}_3$  can be seen to have separated.

Another mixture system that is even more challenging than the  $\text{MoO}_3/\text{Al}_2\text{O}_3$  system was also considered. Accordingly, comparative experiments (REHPS, MAIM and solvent-based mixing) were conducted with a mixture of Cu and  $\text{TiO}_2$ , and the results are shown in Fig. 7. The calculated elemental ratio of Cu/Ti is 1.3333. EDX spot analysis indicates that the standard deviation of the REHPS sample is 0.210 and the frequency distribution for the REHPS sample is reasonably good with one major peak. Unfortunately, the peak does not correspond to the theoretical value for the mixture and, clearly, these results are much worse than the results for  $\text{Al}_2\text{O}_3/\text{SiO}_2$  or  $\text{Al}_2\text{O}_3/\text{MoO}_3$  mixtures.

The mixing of Cu and  $\text{TiO}_2$  was also poor using the solvent-based system and the MAIM system, as shown in Fig. 7. While the standard deviation for MAIM is quite good, the actual mixing is poor, as the peak does not correspond to the

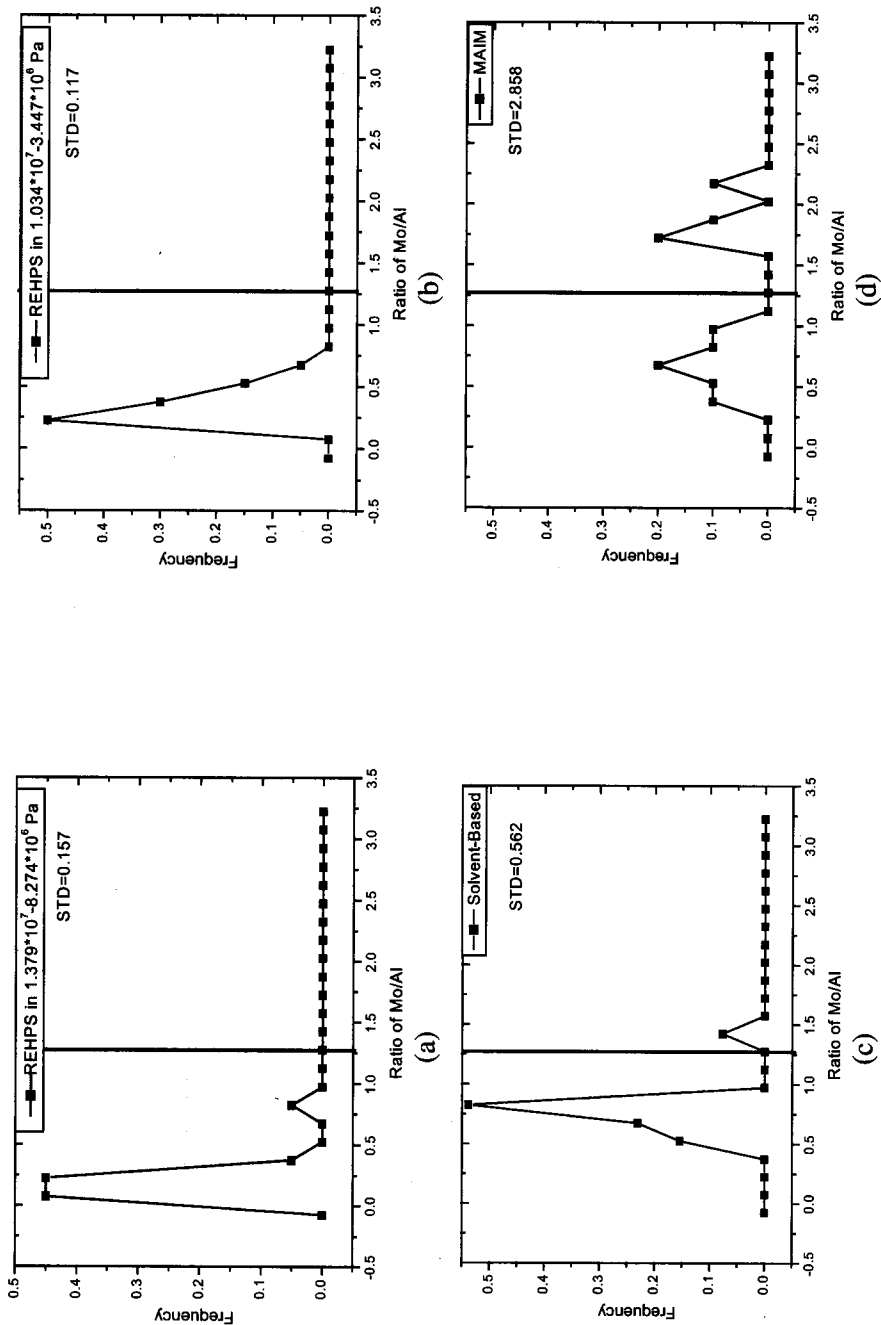


**Figure 5.** EDX spot analysis results of the mixtures of  $\text{MoO}_3/\text{Al}_2\text{O}_3$  (1 : 1). Results for (a) REHPS, released while pressure in the chamber dropped from  $1.379 \times 10^7$  down to  $8.274 \times 10^6$  Pa, (b) REHPS, released while pressure in the chamber dropped from  $1.034 \times 10^7$  down to  $3.447 \times 10^6$  Pa, (c) solvent-based mixing and (d) MAIM mixing.



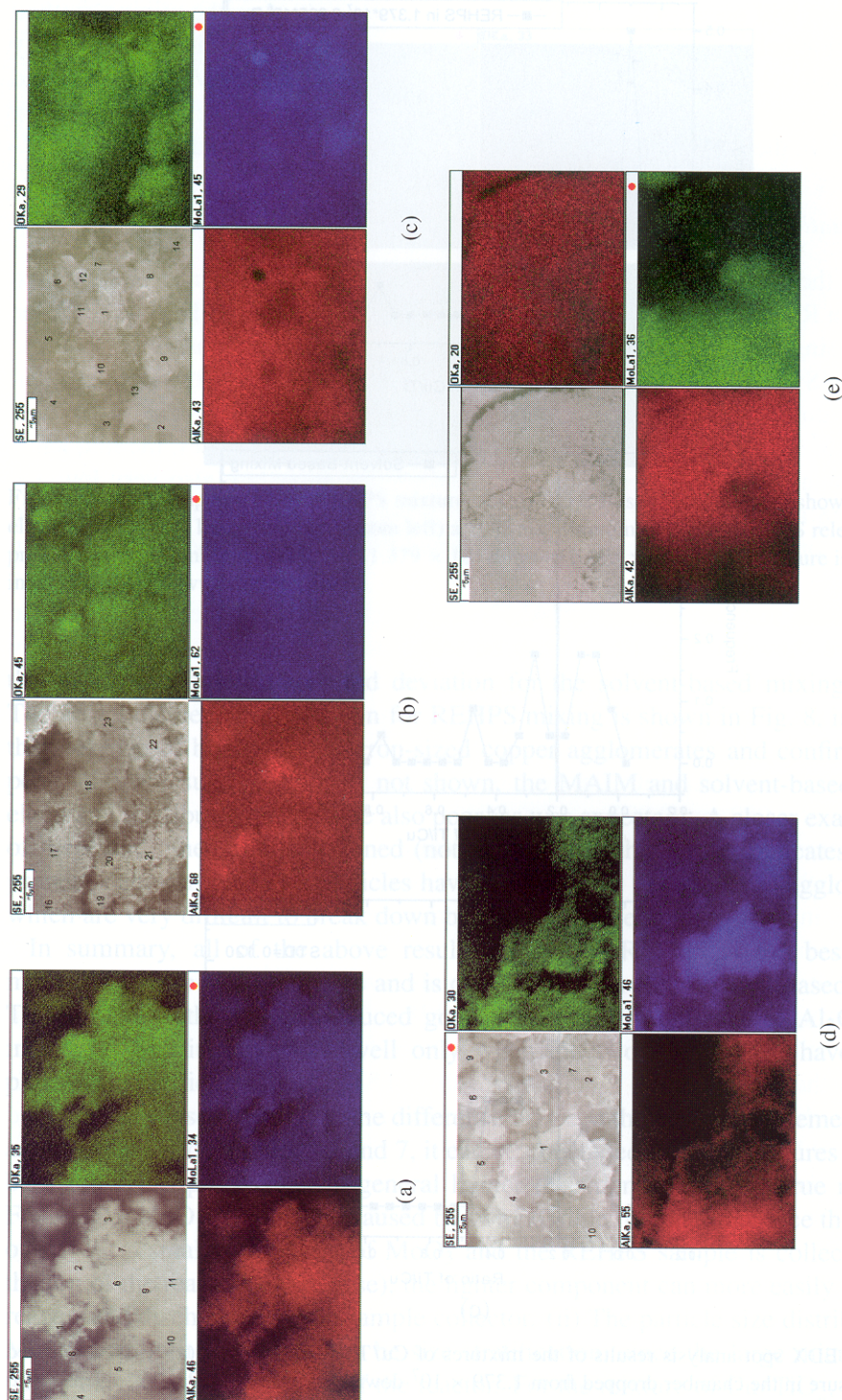


**Figure 6.** EDX mapping of the mixtures of  $\text{Al}_2\text{O}_3/\text{MoO}_3$ . Results in each case show secondary electron image (top left), Al map (bottom left) and Mo map (bottom right) for (a) REHPS released while pressure in the chamber dropped from  $1.379 \times 10^7$  down to  $8.274 \times 10^6$  Pa, (b) REHPS released while pressure in the chamber dropped from  $1.034 \times 10^7$  down to  $3.447 \times 10^6$  Pa, (c) solvent-based mixing, (d) MAIM mixing and (e) hand-mixing. This figure is published in colour on <http://www.ingenta.com>.

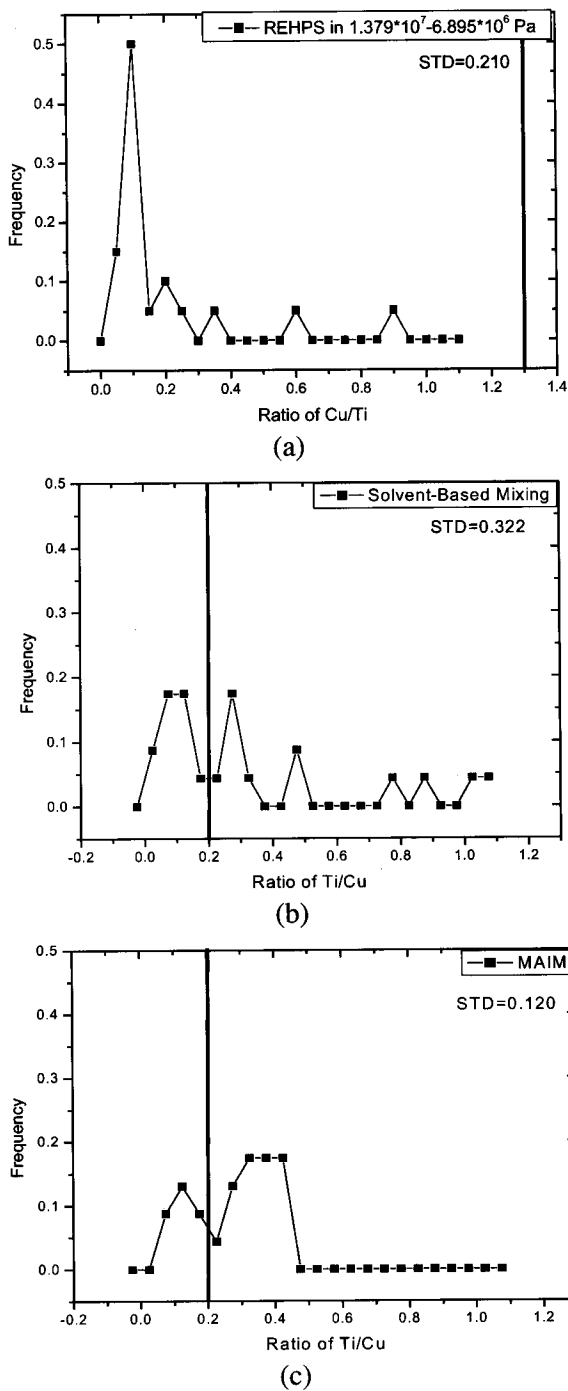


**Figure 7.** EDX spot analysis results of the mixtures of Cu/TiO<sub>2</sub>. Results for (a) REHPS released while pressure in the chamber dropped from  $1.379 \times 10^7$  down to  $6.895 \times 10^6$  Pa, (b) solvent-based mixing and (c) MAIM mixing.



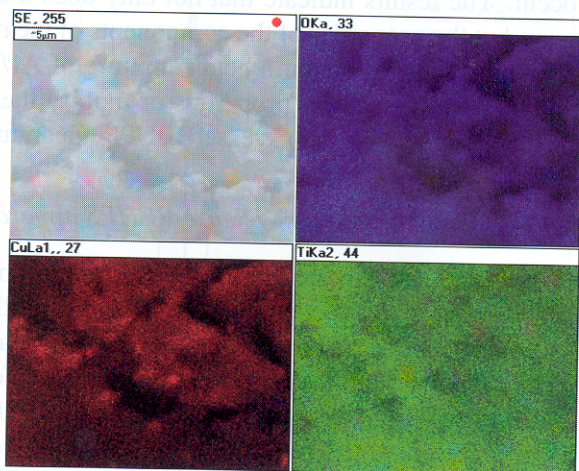


**Figure 8.** EDX mapping of the REHPS mixture of Cu/TiO<sub>2</sub>. Results in each case show secondary electron image (top left), Cu map (bottom left) and Ti map (bottom right) for REHPS released while pressure in the chamber dropped from  $1.379 \times 10^7$  down to  $6.895 \times 10^6$  Pa. This figure is published in colour on <http://www.ingenta.com>.

theoretical value. The standard deviation for the solvent-based mixing is poor. The actual elemental distribution for REHPS mixing is shown in Fig. 8, indicating the presence of big several micron-sized copper agglomerates and confirming the poor mixing results. Although not shown, the MAIM and solvent-based mixing elemental distribution results are also poor (as was expected). A closer examination of these and other results obtained (not presented in this paper) indicates that the primary nano-sized copper particles have formed large micron-sized agglomerates, which are very difficult to break down by REHPS processing.

In summary, all of the above results show that REHPS is the best mixing method for nano-sized particles and is definitely better than solvent-based mixing. The MAIM method only produced good results for the mixture of Al<sub>2</sub>O<sub>3</sub>/SiO<sub>2</sub>, indicating that it may work well only when the two constituents have similar physical properties.

By paying close attention to the difference between the calculated elemental ratio and experiment data in Figs 5 and 7, it can be concluded that the mixtures obtained by the REHPS process are in general lighter (less dense) than the true mixtures. For Al<sub>2</sub>O<sub>3</sub>/MoO<sub>3</sub> this may be caused by two possible reasons. (i) Since the density of Al<sub>2</sub>O<sub>3</sub> is smaller than that of MoO<sub>3</sub> and the REHPS sample is collected from the top of the reactor (top release), the lighter component can more easily leave the reactor and discharge into the sample collector. (ii) The particle size distribution of MoO<sub>3</sub> is uneven and there may be size stratification, since the large micron-sized flakes may stay at the bottom of the reactor. For the mixture of Cu/TiO<sub>2</sub>, since the copper particles are much heavier and larger than the titania particles, density-based

stratification will occur. The results indicate that not only does the mixing method affect mixing behavior, but the properties of the components of the mixture also play an important role as well. Thus, to obtain a better mixture of  $\text{Al}/\text{MoO}_3$ , we need to mix two nano-particles having similar properties or modify the REHPS mixing procedure. In the next section, the bottom-release REHPS apparatus is considered.

#### 4.2. Evaluation of mixing methods: Bottom-release REHPS apparatus

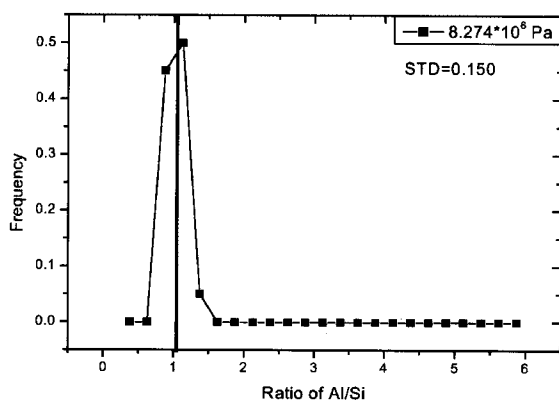
Based on the above results, it appears that the mixing efficiency may be improved by using a REHPS apparatus where the sample is released from the bottom of the vessel. Using our second REHPS mixing apparatus (bottom release), we repeated the  $\text{Al}_2\text{O}_3/\text{SiO}_2$  experiments and the results are shown in Fig. 9 for three different operating conditions (pressure in the reactor =  $8.274 \times 10^6$ ,  $1.379 \times 10^7$  and  $2.068 \times 10^7$  Pa, respectively). As can be seen, for all three pressures, the frequency plots show a single sharp peak and the standard deviations are also very low, i.e. 0.15, 0.138 and 0.155. These results are as good as or better than those obtained using the top-release apparatus and also better than solvent-based mixing shown in Fig. 3.

The results for the mixture of  $\text{Al}_2\text{O}_3/\text{MoO}_3$  processed in the bottom-release system are shown in Fig. 10. As can be seen, these results are also significantly better than those reported for the top-release apparatus and also the solvent-based mixing results in Fig. 5. For each operating condition ( $8.274 \times 10^6$  and  $1.379 \times 10^7$  Pa), there is a single dominant peak in the frequency distribution plots and it also corresponds to the theoretically calculated value ( $\text{Al}/\text{Mo}$ ), with standard deviations of 0.082 and 0.097.

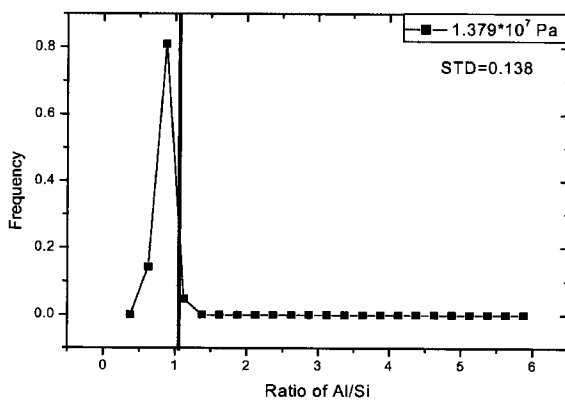
From these results, an important observation is made, i.e. that the operating pressure within the reactor (mixing chamber) does not appear to make a significant difference in the mixing results when the pressure and temperature are above the critical condition.

The results for the mixture of  $\text{Cu}/\text{TiO}_2$  (bottom release) are shown in Fig. 11 for two operating pressures ( $8.274 \times 10^6$  and  $1.138 \times 10^7$  Pa). These results show that mixing is still poor even when using the bottom-release apparatus. The reader is reminded that, as shown in Fig. 7, the results of solvent-based mixing as well as MAIM are both quite poor. In fact, all of these results are not very good, despite the fact that MAIM shows the lowest standard deviation of the mixture. These poor results are due to the presence of large agglomerates of copper nano-particles, which are quite difficult to de-agglomerate since copper nano-particles have a tendency to be sintered with each other. As will be shown in an FESEM image later, primary particles of copper are about 150 nm and they form micron-sized aggregates which appear to be soft-sintered, and hence cannot be de-agglomerated by REHPS.

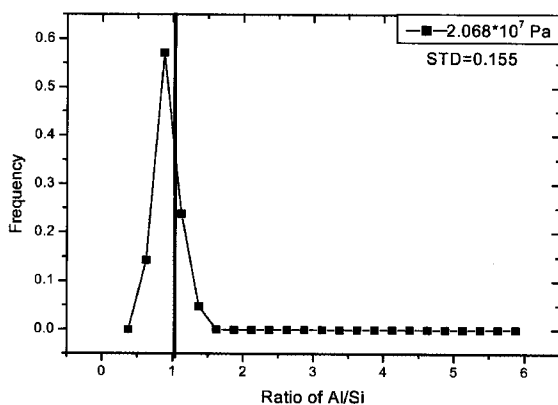
A limited set of results is also shown for mixing using liquid  $\text{CO}_2$  instead of supercritical  $\text{CO}_2$  and the effect of using a smaller nozzle. Figure 12 shows the results for REHPS mixing of the  $\text{Al}_2\text{O}_3/\text{SiO}_2$  system at a pressure and tem-



(a)



(b)



(c)

**Figure 9.** EDX spot analysis result of the REHPS mixture of  $\text{Al}_2\text{O}_3/\text{SiO}_2$  (1 : 1) (by using the bottom-release apparatus). Results for REHPS released in the chamber at a pressure of (a)  $8.274 \times 10^6$ , (b)  $1.379 \times 10^7$  and (c)  $2.068 \times 10^7$  Pa.

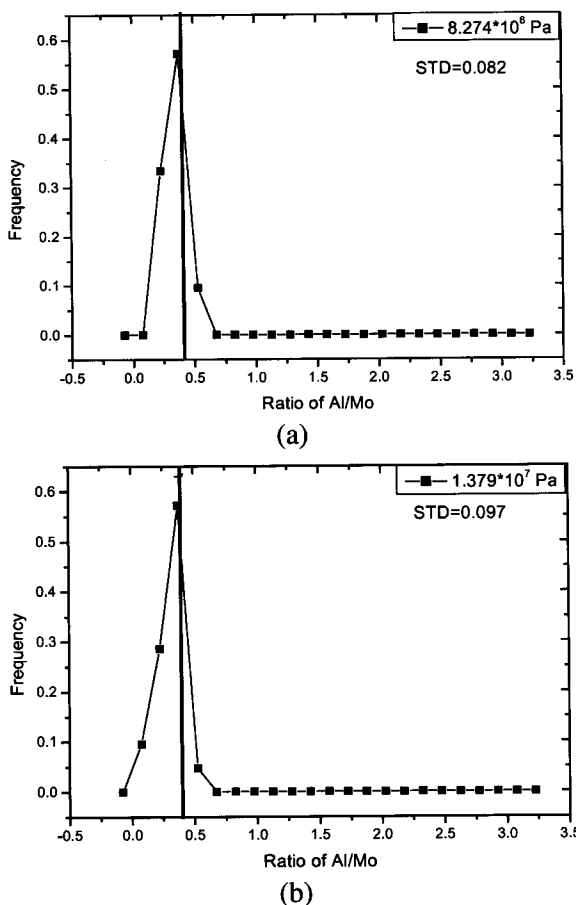


**Figure 10.** EDX spot analysis result of the REHPS mixture of  $\text{Al}_2\text{O}_3/\text{MoO}_3$  (using the bottom-release apparatus). Results for REHPS released in the chamber at a pressure of (a)  $8.274 \times 10^6$  and (b)  $1.379 \times 10^7$  Pa.

perature ( $1.034 \times 10^7$  Pa and  $20^\circ\text{C}$ ) such that liquid  $\text{CO}_2$  is present in the mixing chamber. Once again, a single dominant peak is observed in the frequency distribution plot, indicating good mixing (standard deviation is 0.145). The results for a  $250\text{-}\mu\text{m}$  (instead of a  $500\text{-}\mu\text{m}$ ) expansion nozzle, shown in Fig. 13, indicates that the homogeneity of the mixture is similar to that obtained using the  $500\text{-}\mu\text{m}$  nozzle (Fig. 3a). This implies that the nozzle size probably does not have a significant effect on the mixing quality. It is noted, however, that the results shown in Figs 12 and 13 are preliminary, and more extensive studies are required to make a strong conclusion regarding the effect of liquid media and/or nozzle size. However, as was previously concluded, the preliminary results using liquid  $\text{CO}_2$  indicate that the high-pressure drop expansion is mainly responsible for de-agglomeration and subsequent mixing of the nanoparticles.

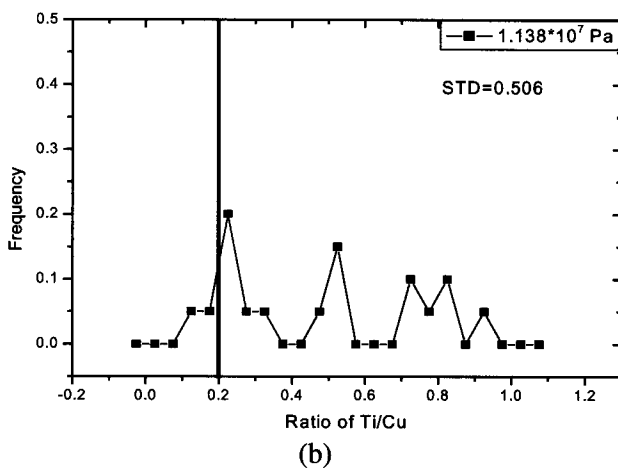
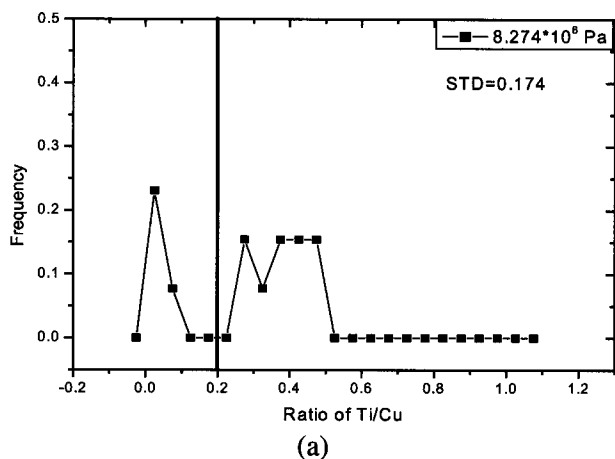


**Figure 11.** EDX spot analysis result of the REHPS mixture of Cu/TiO<sub>2</sub> (using the bottom-release apparatus). Results for REHPS released in the chamber at a pressure of (a)  $8.274 \times 10^6$  and (b)  $1.138 \times 10^7$  Pa.

### 4.3. FESEM evaluation

**4.3.1. Secondary electron image.** Although EDX analysis is a powerful tool for both quantitative analysis as well as mapping the elemental distribution in the mixture, its resolution is limited to a quasi-spherical volume of around  $1 \mu\text{m}$  in diameter. FESEM can provide a very high magnification image at the nano-scale and can be used to determine the mixing behavior at that scale. Generally, a secondary electron image of FESEM with high magnification can be used to distinguish a nano-particle mixture directly if the two constituents have significant size and/or shape differences. Here, several images for the mixture systems considered in the previous section are shown to illustrate the capability of this approach for qualitative evaluation.

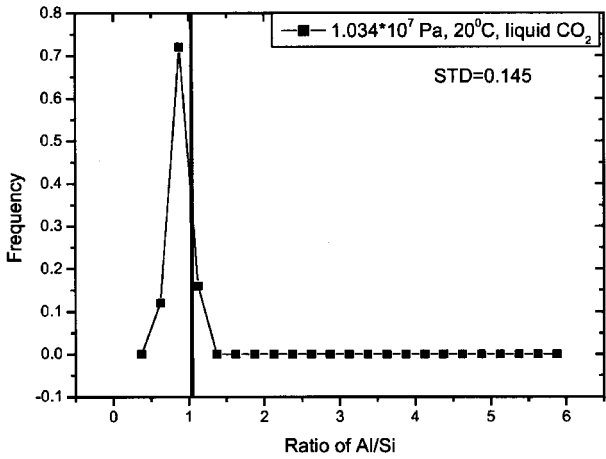


**Figure 12.** EDX spot analysis result of the mixture of Al<sub>2</sub>O<sub>3</sub>/SiO<sub>2</sub> (using the bottom-release apparatus) when the processing fluid is liquid CO<sub>2</sub>.

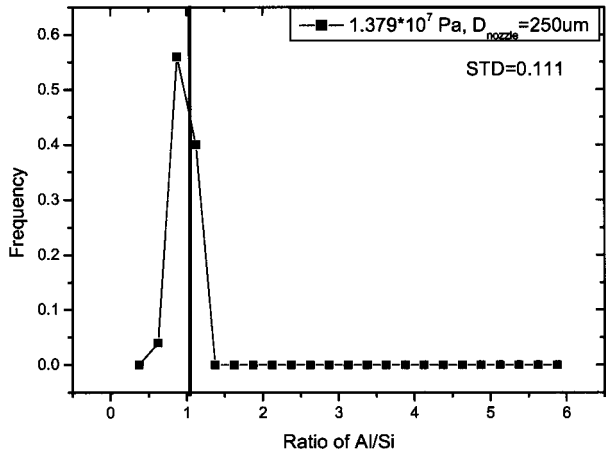


**Figure 13.** EDX spot analysis result of the REHPS mixture of Al<sub>2</sub>O<sub>3</sub>/SiO<sub>2</sub> (using the bottom-release apparatus) with release through a 250-μm nozzle and supercritical CO<sub>2</sub>.

For example, the FESEM images in Fig. 14a show that the MoO<sub>3</sub> particles have many particles shaped like flakes, which can be clearly seen in the mixture of Al<sub>2</sub>O<sub>3</sub>/MoO<sub>3</sub> (Fig. 14d). While these big flakes can be identified in the image, the small MoO<sub>3</sub> particles present in the mixture cannot be easily distinguished at this scale. Similarly, it is very easy to distinguish copper particles (Fig. 14b) in the mixture of Cu/TiO<sub>2</sub> (Fig. 14e), because the size of the copper particles is much larger than the titania particles and copper has a strong secondary electron signal. We can clearly see titania agglomerates among the copper agglomerates. On the other hand, for the mixture of SiO<sub>2</sub>/Al<sub>2</sub>O<sub>3</sub> where the size and shape of SiO<sub>2</sub> (Fig. 14c) and Al<sub>2</sub>O<sub>3</sub> are similar, it is more difficult to clearly distinguish between them, except for the distinct chain-like structure of the SiO<sub>2</sub> particles clearly visible at the

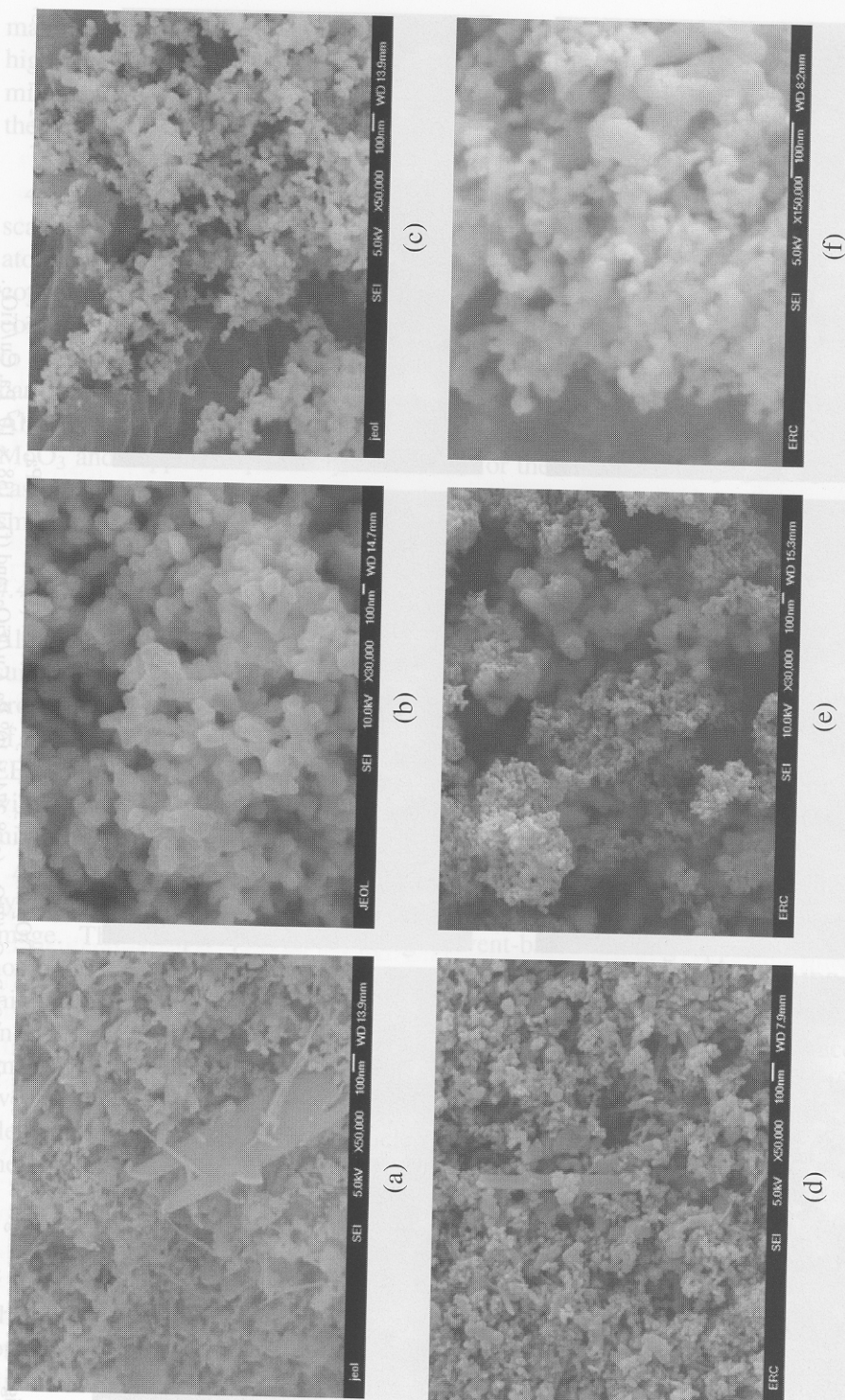


**Figure 14.** FESEM images of nano-particles: (a)  $\text{MoO}_3$ , (b) Cu, (c)  $\text{SiO}_2$  and their mixtures, (d)  $\text{Al}_2\text{O}_3/\text{MoO}_3$ , (e) Cu/ $\text{TiO}_2$ , and (f)  $\text{SiO}_2/\text{Al}_2\text{O}_3$ .



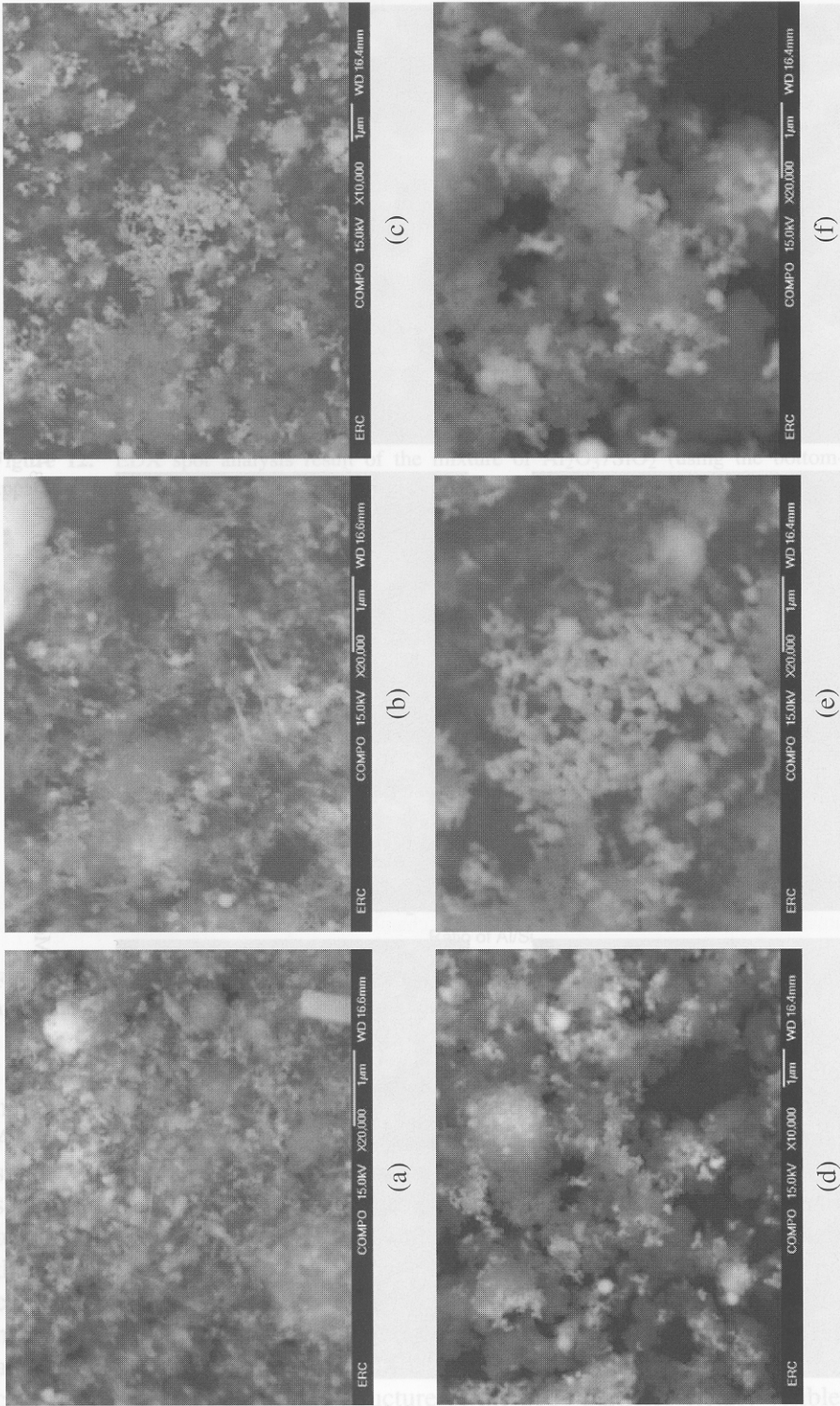


**Figure 15.** BSE images of REHPS mixtures of Cu/TiO<sub>2</sub> and Al<sub>2</sub>O<sub>3</sub>/MoO<sub>3</sub>. Conditions: (a)  $8.274 \times 10^6$  Pa, Al<sub>2</sub>O<sub>3</sub>/MoO<sub>3</sub>, (b)  $1.379 \times 10^7$  Pa, Al<sub>2</sub>O<sub>3</sub>/MoO<sub>3</sub>, (c)  $8.274 \times 10^6$  Pa, Cu/TiO<sub>2</sub>, (d)  $1.138 \times 10^7$  Pa, Cu/TiO<sub>2</sub>, (e)  $8.274 \times 10^6$  Pa, Cu/TiO<sub>2</sub>, and (f)  $1.138 \times 10^7$  Pa, Cu/TiO<sub>2</sub>.



magnification of  $\times 150\,000$  in the mixture of  $\text{SiO}_2/\text{Al}_2\text{O}_3$  (Fig. 14f). Nonetheless, high-resolution FESEM images can only provide a qualitative indication of particle mixing at the nano-scale, and even that is highly dependent on the size and shape of the particles in the mixture.

**4.3.2. Back scattered image.** In addition to secondary electron imaging, back-scattered imaging can also be used to distinguish particles that have different atomic weights. As seen in the back-scattered images in Fig. 15, the  $\text{MoO}_3$  and copper particles are much brighter than the alumina and titania, respectively. When compared with the secondary electron images, the back-scattered images are easier to identify. Since back-scattering electrons reflect signals of nanometer scale, it can be used to identify nano-particles. As seen in the images of the mixtures of  $\text{Al}_2\text{O}_3/\text{MoO}_3$  and  $\text{Cu}/\text{TiO}_2$  in Fig. 15, one can identify the brighter particles of  $\text{MoO}_3$  and copper, respectively. However, for the mixture of  $\text{Al}_2\text{O}_3/\text{SiO}_2$ , it is not easy to obtain a meaningful image contrast since the atomic weight difference is too small to be distinguished.

#### 4.4. EELS/STEM characterization

Although FESEM is capable of distinguishing nano-particles directly, it is only suitable for mixtures with differences in size, shape or some other physical properties like atomic weight. Thus, this technique is not adequate for a mixture of  $\text{SiO}_2/\text{Al}_2\text{O}_3$ . To obtain quantitative information for this nano-particle mixture, EELS with a STEM mode can be used. A LEO 922 in-column energy filtering TEM with scanning mode was utilized for the nano-scale analysis of the  $\text{SiO}_2/\text{Al}_2\text{O}_3$  mixture.

As seen in Fig. 16, the two different types of particles can be clearly distinguished by a comparison of the original zero loss image and the Al element filtered image. The sample processed using solvent-based mixing appears to be less homogeneously mixed at the nano-scale when compared to the REHPS-based mixture. The results shown in Fig. 16 are typical of several samples that were analyzed using EELS. The results indicate that EELS can provide a very accurate image of element distribution at the nano-scale and that REHPS mixing is effective even at the nano-scale. The EELS technique is based on the atomic order of an element, and has no relation to particle size and shape. Thus, it is the most powerful method to characterize a mixture of nano-particles.

## 5. CONCLUDING REMARKS

The objective of this paper was to evaluate the effectiveness of the REHPS process for nano-particle mixing. This was accomplished through analyzing the results of a number of experiments on several nano-particulate systems. Mixing was also carried out using the MAIM process and a solvent-based process for comparison

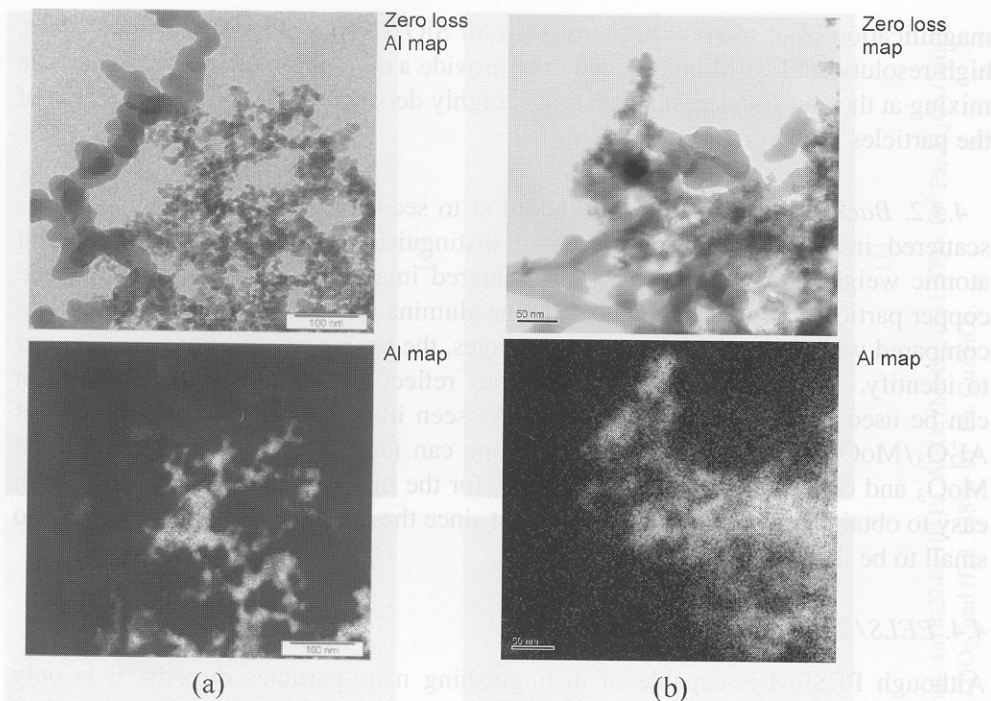


**Figure 16.** EELS images of mixtures of  $\text{Al}_2\text{O}_3/\text{SiO}_2$ : (a) solvent mixing results [zero loss image (top) and Al map (bottom)] and (b) REHPS mixing results [zero loss image (top) and Al map (bottom)].

with the REHPS results. A number of mixture characterization methods were also evaluated.

It is shown that EDX spot analysis is useful for a semi-quantitative analysis at the micron scale, but cannot determine mixing quality at the nanoscale. FESEM may be used for characterization at the nano-scale, but it can only provide qualitative results when a significant difference in size, shape and atomic weight exist between the constituents. It is also shown that EELS, along with STEM, is the most powerful method to characterize nano-particles mixtures as it can map the elemental distribution at nanometer resolution. However, it is an expensive and time-consuming method for obtaining a large amount of statistically significant results.

An analysis of the experimental results by various methods, in particular the EDX spot analysis technique, indicates that REHPS is the best mixing method for nano-particles amongst the three methods studied. It works very well when the two particles mixed are generally similar in size and do not have a wide size distribution, e.g. the mixtures of nano-sized  $\text{Al}_2\text{O}_3$  and  $\text{SiO}_2$  described in this paper. It also works well for a mixture of  $\text{Al}_2\text{O}_3$  and  $\text{MoO}_3$ , even though the  $\text{MoO}_3$  particle size distribution is wide, but the density difference between the two materials is not very large. When the density difference is significant and the agglomerates of one of the constituents are very difficult to break, REHPS mixing does not provide good

results. However, the results obtained using the REHPS method were as good or better than the results obtained using the other mixing methods.

Good mixing by REHPS appears to be due to the rapid pressure expansion of the suspended mixture. It was observed that the samples collected before the rapid expansion were not well mixed, while the samples collected after the rapid expansion were very well mixed. Hence, the sudden decrease in pressure appears to be the major reason for the break-up of agglomerates and subsequent mixing. Overall, the REHPS process is a promising new method for nano-particle mixing.

### Acknowledgements

The authors are grateful to Ms Seibein Kerry (University of Florida) for SEM analysis and to the staff of LEO (USA) who performed EELS analysis for us. Financial support from the US Army, Picatinny Arsenal (contract DAAE30-98-C-1050), the New Jersey Commission of Science and Technology (award 01-2042-007-24) and the National Science Foundation (CTS-9985618 and CTS-0116595) is gratefully acknowledged. Thanks are also due to Dr Herbert Riemenschneider of Degussa Co. for providing some of the nano-powders.

### REFERENCES

1. L. T. Fan, Y. M. Chen and F. S. Lai, Recent developments in solids mixing, *Powder Technol.* **61** (3), 255–287 (1990).
2. K. M. Hill, J. F. Gilchrist, J. M. Ottino, D. V. Khakhar and J. J. McCarthy, Mixing of granular materials: a test-bed dynamical system for pattern formation, *Int. J. Bifurcat. Chaos.* **9** (8), 1467–1484 (1999).
3. N. Imanaka, J. Kohler, T. Masui, G. Y. Adachi, E. Taguchi and H. Mori, Inclusion of nanometer-sized  $\text{Al}_2\text{O}_3$  particles in a crystalline  $(\text{Sc}, \text{Lu})_2(\text{WO}_4)_3$  matrix, *J. Am. Ceramic Soc.* **83** (2), 427–429 (2000).
4. P. G. J. Van der Wel, Powder mixing, *Powder Handling Processing* **11** (1), 83–86 (1999).
5. M. Peciar, Mixing of finely powdered materials, *Chem. Prum.* **42** (5-6), 124–126 (1992).
6. N. Naganuma, Mixing powder with liquid, *Netsu Shori.* **31** (2), 95–99 (1991).
7. O. Vaizoglu, Assessment of the degree of mix of powder mixtures, *Turk. J. Phys.* **23** (1), 97–104 (1999).
8. C. Wightman and F. J. Muzzio, Quantitative characterization of powder blending processes, *AIChE Symp. Ser.* **313**, 71–75 (1996).
9. K. Makino, T. Shoji, M. Sakamoto and M. Nanba, Development of simultaneous measurement of method for powder porosity and mixing ratio in mixing powder and its application, *Sozai Busseigaku Zasshi.* **3** (2), 72–83 (1990).
10. D. Wei, R. N. Dave and R. Pfeffer, Mixing and characterization of nanosized powders: An assessment of different techniques, *J. Nanopart. Res.* **4** (1/2), 21–41 (2002).